Acta Crystallographica Section D
Biological Crystallography
ISSN 0907-4449

Structure of *Escherichia coli* BamB and its interaction with POTRA domains of BamA

Cheng Dong,[a,b]‡ Xue Yang,[a,b]‡ Hai-Feng Hou,[c] Yue-Quan Shen[a,b] and Yu-Hui Dong[c]*

[a]State Key Laboratory of Medicinal Chemical Biology, Nankai University, Tianjin 300071, People's Republic of China, [b]College of Life Sciences, Nankai University, Tianjin 300071, People's Republic of China, and [c]Beijing Synchrotron Radiation Facility, Institute of High Energy Physics, Chinese Academy of Sciences, Beijing 100049, People's Republic of China

‡ These authors made equal contributions.

Correspondence e-mail: dongyh@ihep.ac.cn

Received 4 January 2012
Accepted 21 May 2012

PDB Reference: BamB, 3q54.

In *Escherichia coli*, the BAM complex is essential for the assembly and insertion of outer membrane proteins (OMPs). The BAM complex is comprised of an integral β-barrel outer membrane protein BamA and four accessory lipoproteins BamB, BamC, BamD and BamE. Here, the crystal structure of BamB is reported. The crystal of BamB diffracted to 2.0 Å with one monomer in the asymmetric unit and the structure is composed of eight-bladed β-propeller motifs. Pull-down and Western blotting assays indicate that BamB interacts directly with the POTRA 1–3 domain of BamA and the C-terminal region of the POTRA 1–3 domain plays an important role in the interaction, while the POTRA 1–2 domain is not required for the interaction.

1. Introduction

The cell envelope of Gram-negative bacteria is composed of the inner membrane and the outer membrane, which are separated by the periplasm. The outer membrane consists of phospholipids, lipopolysaccharides (LPS) and integral outer membrane proteins (OMPs) (Wu *et al.*, 2005). Omp85 is an essential component in outer membrane biogenesis which can export lipids and assemble outer membrane proteins (Genevrois *et al.*, 2003; Voulhoux *et al.*, 2003). The integral β-barrel membrane proteins are conserved in prokaryotes and eukaryotes. In *Escherichia coli*, the Omp85 homologue BamA, which belongs to the BAM complex, is crucial for outer membrane assembly (Knowles *et al.*, 2009). The nascent OMPs are synthesized in the cytoplasm with an N-terminal signal sequence which can be recognized by the chaperones SecA and SecB, and the OMPs are translocated through the inner membrane into the periplasm by the SecYEG complex. After removal of the signal sequence, the unfolded OMPs are recruited and delivered to the BAM complex by periplasmic chaperones such as SurA, Skp and DegP. The BAM complex folds and inserts the nascent OMPs into the outer membrane, but how it does this is poorly understood (Pugsley, 1993; Bos *et al.*, 2007; Gatsos *et al.*, 2008; Knowles *et al.*, 2009). Understanding the mechanism of each component is highly significant, as it could lead to strategies for devising drugs.

The BAM complex comprises an integral β-barrel outer membrane protein BamA and four accessory lipoproteins BamB, BamC, BamD and BamE (Wu *et al.*, 2005; Sklar *et al.*, 2007). The BAM complex is essential for outer membrane protein assembly (Werner & Misra, 2005; Doerrler & Raetz, 2005), although the specific function of each component is not yet clear. BamA contains N-terminal polypeptide-transport-associated (POTRA) domains and a C-terminal β-barrel domain. The structures of the five POTRA domains, which have a similar basic folding structure β-α-α-β-β, have been determined by X-ray crystallography, NMR and small-angle

X-ray scattering (SAXS); while the POTRA 3 domain has a β-augmentation that is considered to be the protein binding site, the POTRA 5 domain is crucial for interactions with the lipoproteins BamB, BamC, BamD and BamE (Kim *et al.*, 2007; Gatzeva-Topalova *et al.*, 2008, 2010). BamB and BamD make direct interactions with the POTRA domains of BamA, while BamC and BamE indirectly bind to BamA *via* BamD (Malinverni *et al.*, 2006). The BAM complex can be reconstituted from the purified components *in vitro*; the presumed BamA:BamB:BamC:BamD ratio was 1:1:1:1 (Hagan *et al.*, 2010).

BamA and BamD are required for cell viability (Voulhoux *et al.*, 2003; Wu *et al.*, 2005), while BamB, BamC and BamE are nonessential for cell viability and only affect the assembly of some outer membrane proteins (Malinverni *et al.*, 2006; Voulhoux *et al.*, 2003; Wu *et al.*, 2005).

From bioinformatics, mutagenesis and biochemical analysis, it has been shown that deletion of BamB reduces the levels of many OMPs and leads to hypersensitivity to some antibiotics, while the absence of BamB and DegP leads to a synthetic lethal phenotype (Charlson *et al.*, 2006). BamB plays an important role in the assembly of OMPs which are delivered by SurA (Hagan *et al.*, 2010). Moreover, BamB and SurA working together are more important in protein assembly than their individual actions (Ruiz *et al.*, 2005; Onufryk *et al.*, 2005; Hagan *et al.*, 2010).

Residues Leu173, Leu175, Arg176, Asp227 and Asp229 of BamB are crucial for interaction with BamA, while the region Val319–His328 plays an important part in biological function of BamB other than its interaction with BamA (Vuong *et al.*, 2008). Recent studies have shown that BamB directly interacts with POTRA 3 of BamA *via* its β-augmentation and also with POTRA 2, POTRA 4 and POTRA 5 (Kim *et al.*, 2007). In order to better understand the interaction between BamB and BamA and to obtain insight into how the BAM complex functions in the folding and insertion of OMPs, we solved the crystal structure of BamB and tested its interaction with the POTRA domains of BamA *via* pull-down and Western blotting assays *in vitro*.

2. Materials and methods

2.1. Cloning and expression

The coding sequence of BamB (residues 25–392; GenBank accession No. AAC75565.1) was amplified from *E. coli* K-12 genomic DNA using the sense primer 5′-GGC**CATATG**AGCGAAGAAGATGTGGTAAA (the *Nde*I restriction site is shown in bold) and the antisense primer 5′-ACG**GAATTC**TTAACGTGTAATAGAGTACACGGT (the *Eco*RI restriction site is shown in bold). The PCR products were cut with the *Nde*I and *Eco*RI restriction enzymes and cloned into pET28a vector (Novagen; the thrombin protease site was replaced by a PreScission protease site). The recombinant plasmid was transformed into *E. coli* BL21 (DE3) cells. The cells were incubated at 310 K with 50 µg ml^{-1} kanamycin in LB medium, induced at an OD_{600} of 0.6 with a final concentration of 0.1 m*M* isopropyl β-D-1-thiogalactopyranoside (IPTG) at 298 K for 12 h and harvested by centrifugation at 5000 rev min^{-1} for 15 min.

2.2. Protein purification

The cells were suspended in 40 ml lysis buffer (20 m*M* Tris–HCl, 200 m*M* NaCl pH 7.5) and lysed by sonication with 0.1 m*M* phenylmethylsulfonyl fluoride (PMSF), 10 mg ml^{-1} lysozyme. The crude cell lysates were centrifuged at 18 000 rev min^{-1} for 45 min; the supernatant was loaded onto an Ni–NTA column (pre-equilibrated with lysis buffer) and nonspecifically bound proteins were washed out with washing buffer (20 m*M* Tris–HCl, 50 m*M* imidazole, 200 m*M* NaCl pH 7.5). The binding protein was eluted with elution buffer (20 m*M* Tris–HCl, 500 m*M* imidazole, 200 m*M* NaCl pH 7.5). The N-terminal His_6 tag was removed by PreScission protease at 277 K overnight, leaving four additional residues (Gly-Pro-His-Met) at the N-terminus of BamB, and the buffer was changed to low-salt buffer (20 m*M* Tris–HCl, 50 m*M* NaCl pH 7.5) using a desalting column (GE Healthcare). The solution was reloaded onto an Ni–NTA column and the flowthrough was concentrated and passed through an anion-exchange column (pre-equilibrated with low-salt buffer; GE Healthcare). The target protein was eluted with high-salt buffer, concentrated to 10 ml and passed through a Superdex 200 column (GE Healthcare). The purity of the prepared protein was determined by SDS–PAGE and the purified protein was concentrated to ∼16 mg ml^{-1} for crystallization trials.

2.3. Crystallization and X-ray diffraction

BamB was screened for crystallization at 293 K in 96-well plates using crystallization screening kits from Hampton Research including Crystal Screen, Index, PEGRx, PEG/Ion, Natrix, SaltRx and PEG 600/LiCl Grid Screen. A crystal of BamB grew within 4 d *via* the sitting-drop vapour-diffusion technique using 25%(*w*/*v*) PEG 3350, 0.2 *M* lithium sulfate monohydrate, 0.1 *M* bis-Tris pH 5.5 as the reservoir buffer. The crystallization drops consisted of 1 µl protein solution and 1 µl reservoir solution. The selenomethionine (SeMet) derivative was purified and crystallized as described above. The crystals were flash-cooled in liquid nitrogen after soaking in cryoprotectant solutions consisting of the reservoir solution supplemented with 25%(*v*/*v*) glycerol. Data sets were collected from both wild-type and SeMet-substituted crystals at 100 K on station BL17U1 of the Shanghai Synchrotron Radiation Facility (SSRF) at the peak wavelength for Se. The wild-type and SeMet-substituted crystals both belonged to space group *I*222. The wild-type BamB crystals diffracted to 2.0 Å resolution, with unit-cell parameters $a = 49.14$, $b = 121.12$, $c = 133.29$ Å, $\alpha = \beta = \gamma = 90^\circ$. SeMet-substituted BamB crystals diffracted to 2.1 Å resolution, with unit-cell parameters $a = 49.15$, $b = 121.11$, $c = 133.29$ Å, $\alpha = \beta = \gamma = 90^\circ$. Data were processed using *HKL*-2000 (Otwinowski & Minor, 1997).

2.4. Structure determination and refinement

The program *HKL2MAP* (Pape & Schneider, 2004) was used to search for six Se sites and initial phases were then

Table 1
Data-collection and refinement statistics for BamB.

Values in parentheses are for the highest resolution shell.

	Wild-type crystal	SeMet-derivative crystal
Space group	*I*222	*I*222
Unit-cell parameters (Å)	a = 49.15, b = 121.12, c = 133.29	a = 49.15, b = 121.11, c = 133.29
Wavelength (Å)	0.9793	0.9793
Resolution range (Å)	50–2.00 (2.07–2.00)	50–2.10 (2.18–2.10)
Total No. of reflections	498081	564606
No. of unique reflections	25190	23337
Multiplicity	4.5 (1.8)	5.2 (2.2)
R_{merge}† (%)	10.2 (25.0)	10.8 (29.8)
$\langle I/\sigma(I)\rangle$	13.3 (2.2)	16.0 (2.1)
Completeness (%)	92.6 (60.2)	97.8 (88.8)
FOM	—	0.640
Refinement		
R_{cryst}‡ (%)	17.2	
R_{free}‡ (%)	23.1	
R.m.s.d.$_{bond}$§ (Å)	0.007	
R.m.s.d.$_{angle}$§ (°)	1.1	
No. of protein atoms	2620	
No. of ligand atoms	0	
No. of solvent atoms	348	
Ramachandran plot, residues in (%)		
Favoured region	97.4	
Allowed region	2.6	
Outlier region	0	
Average B factor (Å^2)		
Protein	35.37	
Solvent	46.36	

† $R_{cryst} = \sum_{hkl} ||F_{obs}| - |F_{calc}|| / \sum_{hkl} |F_{obs}|$. ‡ R_{free} was calculated as R_{cryst}, but from a test set consisting of 5% of data excluded from refinement. § R.m.s.d. for bonds and angles (Engh & Huber, 1991),

calculated using the *PHENIX* software (Zwart *et al.*, 2008). Model building and refinement were performed using *Coot* (Emsley & Cowtan, 2004) and *PHENIX*. After the initial polyalanine model had been built, iterative refinement was performed against the wild-type data to assign all side chains.

Table 2
Constructions of plasmid sequences.

Plasmid	Residues	Tag
pHGB.HA-P1	Ala21–Arg91	His-HA
pHGB.HA-P1-P2	Ala21–Gly172	His-HA
pHGB.HA-P1-P3	Ala21–Asp264	His-HA
pHGB.HA-P1-P4	Ala21–Asn345	His-HA
pHGB.HA-P1-P5	Ala21–Glu420	His-HA
pET28.GST-BamB	Ser25–Arg392	GST

After several refinement cycles with *PHENIX* and *Coot*, the orientations of the amino-acid side chains and bound water molecules were modelled on the basis of $2F_o - F_c$ and $F_o - F_c$ difference Fourier maps. The final structure had an R_{cryst} value of 17.2% and an R_{free} value of 23.1%. The Ramachandran plot calculated using the program *MolProbity* (Chen *et al.*, 2010) showed that 97.4% of the residues were in most favoured regions, 2.6% of the residues were in allowed regions and no residues were in disallowed regions. Detailed data-collection and refinement statistics are summarized in Table 1. Structural representations were generated by *PyMOL* (DeLano, 2002). Sequence comparison and alignment was performed using *ClustalX* (Thompson *et al.*, 2002) and *ESPript* (Gouet *et al.*, 2003).

2.5. Pull-down and Western blotting experiments

The 1200 bp DNA fragment coding for the POTRA 1–5 domain of BamA (residues Alal21–Glu42; UniProtKB P0A940) was amplified from *E. coli* K-12 genomic DNA using the forward primer 5′-GGC**GGATCC**GCTGAAGGGTTC-GTAGTGAAAGAT (the *Bam*HI restriction site is shown in bold) and the reverse primer 5′-ACG**GAATTC**TTACTCTT-TTACCTTGTAGACGACATC (the *Eco*RI restriction site is shown in bold). The PCR product was digested and ligated

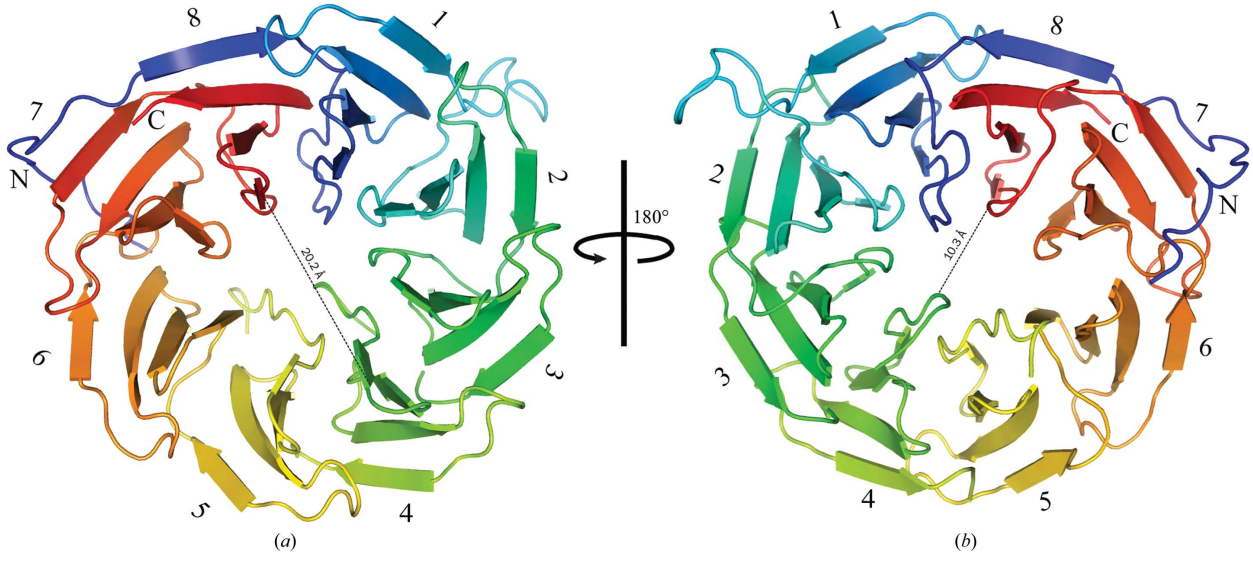

Figure 1
Overall structure of BamB. (*a*) The structure of BamB is composed of eight-bladed β-propellers; each blade motif is shown in a different colour. The diameter of the hole formed by the eight blades is approximately 20 Å at the bottom. (*b*) BamB rotated anticlockwise by 180° about the *y* axis; the diameter of the hole is about 10 Å at the top.

into a modified vector pHGB.HA including a His_6-HA tag at the N-terminus. The plasmid was transformed into *E. coli* BL21 (DE3) for inducible expression. The cells were incubated at 310 K and induced at 298 K overnight using 0.1 m*M* IPTG when the cell density reached an OD_{600} of 0.6. The protein was purified by Ni-affinity chromatography and the elution buffer was exchanged for the experimental buffer (50 m*M* HEPES, 150 m*M* NaCl pH 7.5) using a desalting column (GE Healthcare).

The plasmids for the POTRA 1, POTRA 1–2, POTRA 1–3 and POTRA 1–4 domains were constructed on the basis of the POTRA 1–5 domain of BamA using forward primer 1 (5′-CAGGTAAAAGAACGTTAAACCATTGCCAGCATTAC) and reverse primer 1 (5′-GTAATGCTGGCAATGGTTTA-ACGTTCTTTTACCTG), forward primer 1–2 (5′-GGT-GTTCCAGGAAGGTTAATCAGCTGAAATCCAGC) and reverse primer 1–2 (5′-GCTGGATTTCAGCTGATTAACC-TTCCTGGAACACC), forward primer 1–3 (5′-GAACA-TCACCGAAGGCGATTAATACAAGCTTTCTGGC) and reverse primer 1–3 (5′-GCCAGAAAGCTTGTATTAATCG-CCTTCGGTGATGTTC), and forward primer 1–4 (5′-GTT-GATGCGGGTAACTAATTCTACGTGCGTAAGATC) and reverse primer 1–4 (5′-GATCTTACGCACGTAGAATTAG-TTACCCGCATCAAC), respectively (Table 2). The expression and purification of POTRA 1, POTRA 1–2, POTRA 1–3, POTRA 1–4 were performed using the same protocol as described above for POTRA 1–5.

The gene for BamB encoding residues 25–392 was cloned into a modified vector including a GST tag at the N-terminus and transformed into *E. coli* BL21 (DE3) cells. The cells were incubated at 310 K and induced at 298 K using 0.1 m*M* IPTG overnight. GST-BamB was purified by GST-affinity chromatography and the elution buffer was exchanged for the experimental buffer 50 m*M* HEPES, 150 m*M* NaCl pH 7.5 using a desalting column (GE Healthcare).

The purified GST-fusion protein (GST-BamB) and the purified HA-fusion proteins (HA-POTRA 1, HA-POTRA 1–2, HA-POTRA 1–3, HA-POTRA 1–4 and HA-POTRA 1–5; equivalent numbers of moles) were incubated in 800 µl reaction buffer consisting of 50 m*M* HEPES, 150 m*M* NaCl pH 7.5, 0.8% Triton X-100, 8% glycerol by rotating at 277 K for 2 h and immobilized on 20 µl Glutathione-Sepharose 4B beads (GE Healthcare) pre-equilibrated with the same reaction buffer for 1 h. The beads were washed six times with reaction buffer and the bound proteins were released from the GST beads by heating at 360 K for 10 min in the presence of 20 µl SDS loading buffer. The supernatant was subjected to SDS–PAGE and detected by Western blotting with anti-HA antibodies (Sigma).

3. Results and discussion

3.1. The overall structure of BamB

The final model contains residues 25–392 of BamB, with the exceptions of residues Met189–Ser193 and Gln234–Asp242, which could not be traced in the electron-density map. The N-terminal sequence 1–23 was predicted to be a signal peptide that anchors the outer membrane. The overall structure consists of eight-bladed β-propellers. Each blade contains four β-sheets connected by four loops (L1-β1-L2-β2-L3-β3-L4-β4; Fig. 2*b*). The eight-bladed β-propellers connect in turn to form a hole (∼20 Å at the bottom and ∼10 Å at the top) in the middle. Blade 8 consists of the C-terminus (β1-β2-β3) and the N-terminus (β4) (Fig. 1).

Superposition of the eight β-propeller motifs shows that the overall structure is similar except for loop 1 of each blade, which is relatively flexible (Fig. 2*a*). Loop 1 of blade 2 is particularly protuberant (Fig. 2*b*) and the projections (Lys100–Leu111) on the top of the overall structure are not conserved or do not exist in other species.

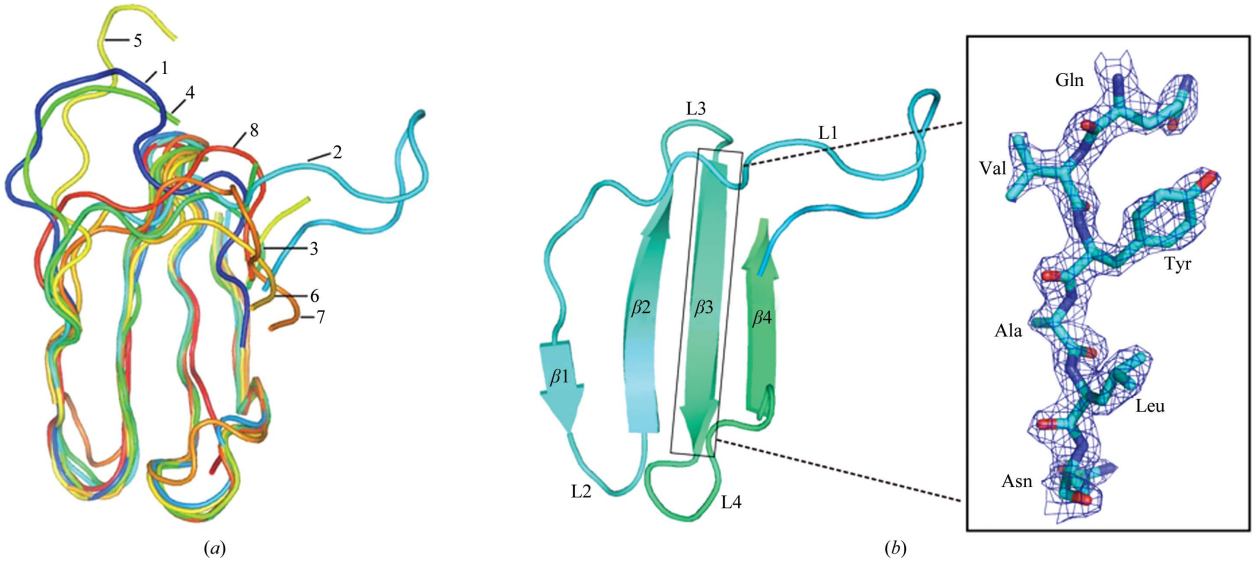

Figure 2
Comparison of each blade motif. (*a*) Superposition of each blade β-propeller, with each blade shown in a different colour as in Fig. 1. (*b*) Ribbon diagram of blade 2 and the order of secondary-structure elements (L1-β1-L2-β2-L3-β3-L4-β4) with an electron-density map of β3.

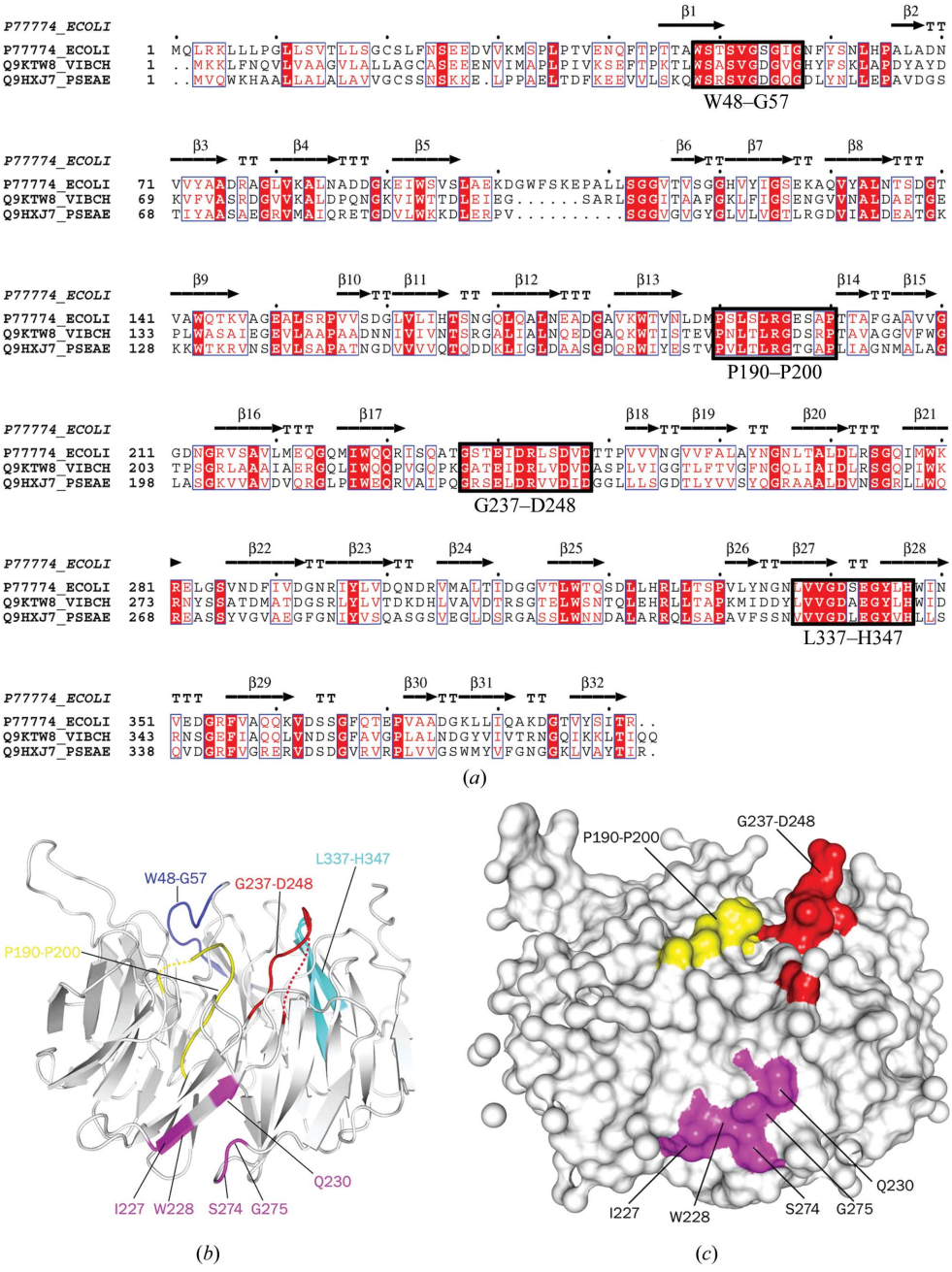

Figure 3
Conserved resides of BamB homologues in Gram-negative bacteria. (*a*) Sequence alignment of BamB homologues in other Gram-negative bacteria. The protein sequences were acquired from the UniProtKB database: P77774 (*E. coli*), Q9KTW8 (*V. cholerae*) and Q9HXJ7 (*P. aeruginosa*). (*b*) Mapping the conserved regions in the ribbon diagram of BamB. (*c*) The highly conserved loops and the residues which accumulated on the surface are shown for the BamB structure.

3.2. The conserved amino acids and the critical residues for BamA interaction

A homology sequence alignment (of sequences from *E. coli*, *Vibrio cholerae* and *Pseudomonas aeruginosa*) shows that there are four conserved regions (Trp48–Gly57, Pro190–Pro200, Gly240–Asp248 and Leu337–His347; Fig. 3). In our structure, loop 1 of blade 4 and loop 1 of blade 5 are two conserved regions that contain crucial residues for binding BamA, such as Leu192, Leu194, Arg195, Asp246 and Asp248 (Charlson *et al.*, 2006), but as electron-density maps were not obtained for these two regions we presume that they are flexible owing to the absence of the POTRA domains of BamA and that the missing regions are crucial for the binding of BamB and BamA.

Mapping all of the highly conserved resides in the structure of BamB, we found that most of the highly conserved resides are not located on the protein surface, suggesting that these highly conserved resides are important for BamB biogenesis, while other highly conserved resides such as Ile227, Trp228, Gln230 (β4 of blade 4), Ser274 and Gly275 (loop 4 of blade 5) accumulate on the surface of BamB (Fig. 3*c*). In particular, β4 of blade 4 located between loop 1 of blade 4 and loop 1 of blade 5 may conveniently provide some binding sites for the POTRA 3 domain *via* its β-augmentation (Fig. 3*c*).

3.3. Pull-down and Western blotting assays to detect the interaction between BamB and the POTRA domains of BamA

Which of the POTRA domains of BamA are able to interact with BamB is a very important question. Therefore, we performed pull-down and Western blotting assays to explore this.

We prepared five N-terminally His_6-HA-tagged BamA POTRA domain constructs (His_6-HA-POTRA 1, His_6-HA-POTRA 1–2, His_6-HA-POTRA 1–3, His_6-HA-POTRA 1–4 and His_6-HA-POTRA 1–5; Fig. 4*b*); all five constructs were expressed in *E. coli* strain BL21 (DE3) and purified by Ni-affinity chromatography. As the same time, we constructed an N-terminally GST-tagged BamB (25–392) plasmid, which was also expressed in *E. coli* BL21 (DE3) and purified by GST-affinity chromatography.

We incubated purified GST-BamB (25–392) and the various POTRA domains of BamA (POTRA 1, POTRA 1–2, POTRA 1–3, POTRA 1–4 and POTRA 1–5) in 50 m*M* HEPES, 150 m*M* NaCl pH 7.5, 0.8% Triton X-100, 8% glycerol at 277 K for 2 h and pulled down the five constructed domains of

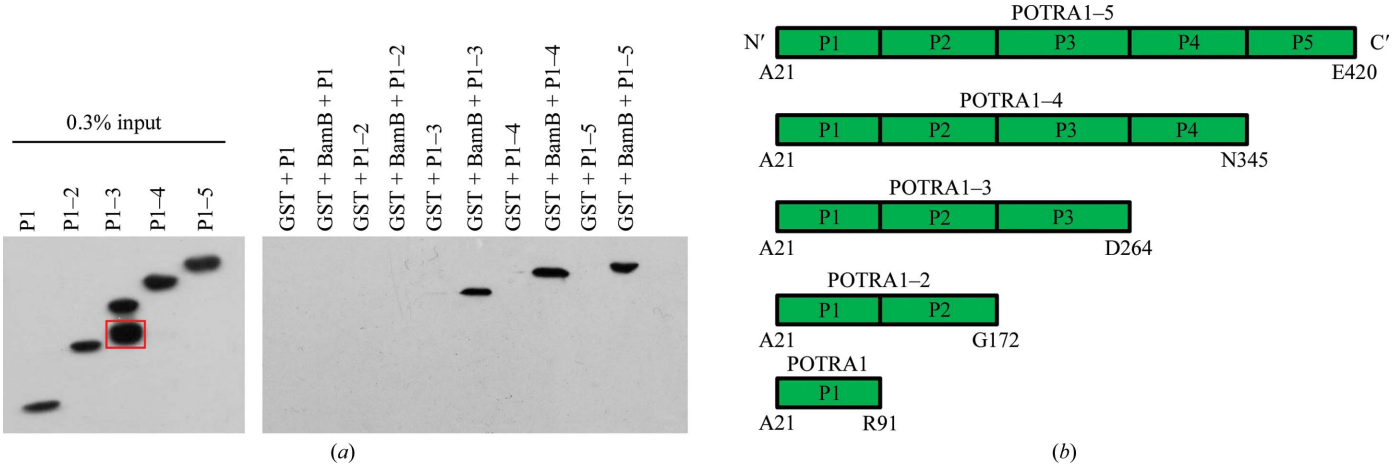

Figure 4
Pull-down and Western blotting assays performed to detect the interaction between BamB (25–392) and the POTRA 1, POTRA 1–2, POTRA 1–3, POTRA 1–4 and POTRA 1–5 domains of BamA. (*a*) The GST-fusion protein (GST-BamB) was used to pull down HA-fusion proteins (HA-P1, HA-P1-2, HA-P1-3, HA-P1-4 and HA-P1-5). The POTRA 1–3 domain protein is unstable and degrades from the C-terminus; the degradation protein in the POTRA 1–3 domain lane is indicated by a red square. (*b*) Summary of the POTRA domains in the BamA truncations.

BamA *via* the GST-fusion protein (GST-BamB); the results were detected by Western blotting with anti-HA antibodies.

The results showed that BamB could pull down POTRA 1–3, POTRA 1–4 and POTRA 1–5, but not POTRA 1 or POTRA 1–2 (Fig. 4*a*), which suggests that POTRA 1–2 is not required for interaction. The POTRA 1–3 domain protein is not very stable and degrades from the C-terminus (Fig. 4*a*, red circle). However, BamB could not pull down degraded POTRA 1–3, which demonstrates that BamB interacts directly with POTRA 1–3 and that the C-terminal region of POTRA 1–3 plays an important role in the interaction.

In summary, BamB consists of eight-bladed β-propeller motifs and the structure of each blade is similar, with the exception of loop 1. The Pro190–Pro200 and Gly237–Asp248 loops are very flexible and are important for binding BamA. The pull-down assay suggested that BamB interacts directly with the C-terminal region of the POTRA 1–3 domain. The POTRA 1–2 domain is not necessary for interaction with BamB.

This work was supported by grants from the Natural Science Foundation of China (grant No. 30900227).

References

Bos, M. P., Robert, V. & Tommassen, J. (2007). *Annu. Rev. Microbiol.* **61**, 191–214.
Charlson, E. S., Werner, J. N. & Misra, R. (2006). *J. Bacteriol.* **188**, 7186–7194.
Chen, V. B., Arendall, W. B., Headd, J. J., Keedy, D. A., Immormino, R. M., Kapral, G. J., Murray, L. W., Richardson, J. S. & Richardson, D. C. (2010). *Acta Cryst.* D**66**, 12–21.
DeLano, W. L. (2002). *PyMOL*. http://www.pymol.org.
Doerrler, W. T. & Raetz, C. R. (2005). *J. Biol. Chem.* **280**, 27679–27687.
Emsley, P. & Cowtan, K. (2004). *Acta Cryst.* D**60**, 2126–2132.
Engh, R. A. & Huber, R. (1991). *Acta Cryst.* A**47**, 392–400.
Gatsos, X., Perry, A. J., Anwari, K., Dolezal, P., Wolynec, P. P., Likić, V. A., Purcell, A. W., Buchanan, S. K. & Lithgow, T. (2008). *FEMS Microbiol. Rev.* **32**, 995–1009.
Gatzeva-Topalova, P. Z., Walton, T. A. & Sousa, M. C. (2008). *Structure*, **16**, 1873–1881.
Gatzeva-Topalova, P. Z., Warner, L. R., Pardi, A. & Sousa, M. C. (2010). *Structure*, **18**, 1492–1501.
Genevrois, S., Steeghs, L., Roholl, P., Letesson, J. J. & van der Ley, P. (2003). *EMBO J.* **22**, 1780–1789.
Gouet, P., Robert, X. & Courcelle, E. (2003). *Nucleic Acids Res.* **31**, 3320–3323.
Hagan, C. L., Kim, S. & Kahne, D. (2010). *Science*, **328**, 890–892.
Kim, S., Malinverni, J. C., Sliz, P., Silhavy, T. J., Harrison, S. C. & Kahne, D. (2007). *Science*, **317**, 961–964.
Knowles, T. J., Scott-Tucker, A., Overduin, M. & Henderson, I. R. (2009). *Nature Rev. Microbiol.* **7**, 206–214.
Malinverni, J. C., Werner, J., Kim, S., Sklar, J. G., Kahne, D., Misra, R. & Silhavy, T. J. (2006). *Mol. Microbiol.* **61**, 151–164.
Onufryk, C., Crouch, M.-L., Fang, F. C. & Gross, C. A. (2005). *J. Bacteriol.* **187**, 4552–4561.
Otwinowski, Z. & Minor, W. (1997). *Methods Enzymol.* **276**, 307–326.
Pape, T. & Schneider, T. R. (2004). *J. Appl. Cryst.* **37**, 843–844.
Pugsley, A. P. (1993). *Microbiol. Rev.* **57**, 50–108.
Ruiz, N., Falcone, B., Kahne, D. & Silhavy, T. J. (2005). *Cell*, **121**, 307–317.
Sklar, J. G., Wu, T., Gronenberg, L. S., Malinverni, J. C., Kahne, D. & Silhavy, T. J. (2007). *Proc. Natl Acad. Sci. USA*, **104**, 6400–6405.
Thompson, J. D., Gibson, T. J. & Higgins, D. G. (2002). *Curr. Protoc. Bioinformatics*, pp. 2.3.1–2.3.22.
Voulhoux, R., Bos, M. P., Geurtsen, J., Mols, M. & Tommassen, J. (2003). *Science*, **299**, 262–265.
Vuong, P., Bennion, D., Mantei, J., Frost, D. & Misra, R. (2008). *J. Bacteriol.* **190**, 1507–1517.
Werner, J. & Misra, R. (2005). *Mol. Microbiol.* **57**, 1450–1459.
Wu, T., Malinverni, J., Ruiz, N., Kim, S., Silhavy, T. J. & Kahne, D. (2005). *Cell*, **121**, 235–245.
Zwart, P. H., Afonine, P. V., Grosse-Kunstleve, R. W., Hung, L.-W., Ioerger, T. R., McCoy, A. J., McKee, E., Moriarty, N. W., Read, R. J., Sacchettini, J. C., Sauter, N. K., Storoni, L. C., Terwilliger, T. C. & Adams, P. D. (2008). *Methods Mol. Biol.* **426**, 419–435.